Tuning the conductance of molecular junctions: Transparent versus tunneling regimes

J. Ferrer
Departamento de Física, Universidad de Oviedo, 33007 Oviedo, Spain

V. M. García-Suárez
Department of Physics, Lancaster University, Lancaster LA1 4YB, United Kingdom

(Received 10 October 2008; revised manuscript received 25 February 2009; published 24 August 2009)

We present a theoretical study of the transport characteristics of molecular junctions, where first-row diatomic molecules are attached to (001) gold and platinum electrodes. We find that the conductance of all of these junctions is on the order of the conductance quantum unit G_0, spelling out that they belong to the transparent regime. We further find that the transmission coefficients show wide plateaus as a function of the energy, instead of the usual sharp resonances that signal the molecular levels in the tunneling regime. We use Caroli's model to show that this is a rather generic property of the transparent regime of a junction, which is driven by a strong effective coupling between the delocalized molecular levels and the conduction channels at the electrodes. We analyze the transmission coefficients and chemical bonding of gold/benzene and gold/benzene-dithiolate junctions to understand why the latter show large resistances while the former are highly conductive.

DOI: 10.1103/PhysRevB.80.085426 PACS number(s): 73.63.Rt, 73.40.−c

I. INTRODUCTION

The field of molecular electronics was arisen by the early realization that organic molecules could act as rectifiers[1] when attached to conducting electrodes to form tunnel junctions. Many experiments with a large variety of organic molecules have been performed,[2,3] typically finding values of the conductance G several orders of magnitude smaller than G_0 ($G_0=2e^2/h$ is the conductance quantum) and a large variability, which hinder the reproducibility of the experiments. Molecular junctions can be understood in terms of resonant tunneling models,[4] where the conduction is carried through the highest occupied molecular orbital and lowest unoccupied molecular orbital (HOMO and LUMO, respectively). These are revealed as sharp resonances in either the densities of states (DOSs) of the molecule or the transmission coefficients $\mathcal{T}(E)$ of the junction and are usually located 1 or 2 eV above or below the Fermi level of the molecule, respectively. Conductance values on the order of G_0 can only be achieved by pinning one of those resonances to the Fermi level of the electrodes. Otherwise, the conductance is very low.

The invention of the scanning tunneling microscope[5] allowed the fabrication of stable atomic point contacts.[6–10] These junctions were found to be highly transparent in many cases and to show values of the conductance on the order of G_0, which confirmed early theoretical predictions on the matter.[11,12] Theoretical analyses of these junctions found that their transmission coefficients $\mathcal{T}(E)$ show wide plateaus as a function of the energy E of the incoming electrons with heights of order 1. The high transparency of these junctions is due to the good matching between the conduction channels at the electrodes and those at the molecule. The (contact) resistance of the junction is different from zero because of the different number of channels at the electrodes and the junction which leads to a recombination of the former to match the later.[4,11]

Importantly, more recent developments using mechanically controllable break junction (MCBJ) techniques demonstrated that high values of the conductance ($\sim G_0$) are not restricted to atomic constrictions but could also be obtained even when platinum or palladium electrodes are bridged by hydrogen molecules.[13,14] These results were reproduced by theoretical simulations,[15,16] which also showed how the antibonding level of the hydrogen molecule hybridized strongly with the conduction channels of the electrodes, providing a junction with a single conduction channel. The transparency of this channel was manifested in the transmission coefficients $\mathcal{T}(E)$ that had a wide plateau of height 1. Furthermore, very recent experimental work confirms that junctions comprising platinum electrodes and either simple benzene[17] or a number of small molecules[18] show conductance values on the order of G_0.

As stated above, junctions in the tunneling regime can shed conductance values of order G_0 provided that a molecular level is exactly pinned to the Fermi energy. But it is hard to believe that all of the junctions discussed in those recent experiments[17,18] display this pinning mechanism. Instead, they clearly indicate that highly transparent molecular junctions can be fabricated with relative ease. They also indirectly hint that thiol capping necessarily leads to junctions in the tunneling regime.

We have performed a number of transport simulations[19] of molecular junctions where first-row diatomic molecules are sandwiched by semi-infinite (001) gold and platinum electrodes with our code SMEAGOL.[20] Our simulations confirm that this type of junctions is highly conductive. Indeed, the transmission coefficients do not show resonant behavior but wide plateaus of height of order 1 instead. To sustain theoretically these simulations, we argue that the conductive behavior of a junction is determined by two factors. First, by the conjugation nature of the molecule, e.g., whether the HOMO and LUMO levels are delocalized throughout the whole molecule or not. Second, by the strength of the chemical bond between the conduction channels at the electrodes and these delocalized HOMO or LUMO. A junction will be highly conductive provided that its molecule is conjugated

and the chemical bond referred above is strong.

Conjugated molecules are reasonably well approximated by Caroli's model.[21] We use this model below to show that when the chemical bond between the delocalized HOMO or LUMO and the conduction channels is strong, the transmission coefficients show wide plateaus whose height is on the order of G_0. We argue that these plateaus are robust against changes in the energy of the HOMO/LUMO levels so that there is no need to fine tune their position to the Fermi level of the electrodes in order to achieve large conductance values. On the contrary, when the conduction channels at the electrodes do not bind chemically with neither the HOMO nor the LUMO levels then the junction is in the tunneling regime where it shows resonant behavior.

Diatomic or triatomic molecules are sufficiently small to show conjugation. Likewise, benzene-based molecules are archetypical conjugated molecules, where the conjugation is driven by internal π bonding. It is therefore important to understand unequivocally why benzene-dithiolate (BDT)/gold junctions show strong tunneling behavior while on the contrary the simpler benzene/gold junctions are highly transparent. We perform below a study of the transmission coefficients of these junctions. Our study indicates that direct Au-S bonding is detrimental of their conductive behavior.

II. SIMULATIONS OF FIRST-ROW DIATOMIC MOLECULES CONTACTED TO (001) GOLD AND PLATINUM ELECTRODES

We have performed simulations of the conductance of (001) gold and platinum junctions that are bridged by diatomic molecules of the first-row elements, using our code SMEAGOL.[20] SMEAGOL is a transport program which uses the nonequilibrium Green's functions formalism[4] to compute the charge density and current of the junction. The Hamiltonian of the junction is determined by discrete Fourier transform theory via the code SIESTA.[22]

We distinguished two clear cases in our study, depending on whether the aim was to map the *ab initio* simulations to the simple model or to do more realistic simulations that can be compared with experiments. In the first case we used gold since it has only *s* states at the Fermi level and gives results that are easy to interpret. We took for simplicity a flat surface, oriented the molecules perpendicular to it, and set the electrode-molecule distance equal to the equilibrium distance of the gold-H_2 junction. In contrast, we used for platinum a more realistic geometry, motivated by the recent experiments by Tal *et al.*[18] We placed in these cases a pyramid of platinum atoms on top of the flat surfaces, as in our earlier publications.[15] We oriented the molecules in a variety of angles, including the bridge, perpendicular and tilted orientations. We finally relaxed the forces of the atoms at the pyramids and molecules. We found in this respect that Li_2, Be_2, B_2, C_2, and N_2 relax to the bridge position while O_2, F_2, and CO relax to a tilted orientation. The perpendicular configuration is stable for some molecules when the distance between leads is very small but such distance does not correspond to the most stable separation.

Our code computes the conductance of the junction via the formula

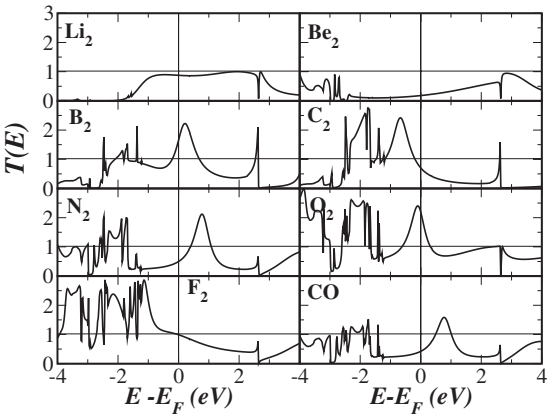

FIG. 1. Transmission coefficients at zero voltage as a function of energy $\mathcal{T}(E)$ for a number of first-row diatomic molecules and CO attached to (001) gold electrodes. The zero of energies corresponds to the position of the Fermi energy of the electrodes at zero voltage. The distance between the last gold atoms at the electrodes and the molecules is set to the equilibrium distance for the gold-H_2 junction (1.5 Å).

$$G(V) = \frac{dI_{leads}(V)}{dV} = G_0 \frac{d}{d(-eV)} \int d\omega T(E = \hbar\omega, V)(n_L - n_R), \tag{1}$$

where $T(E,V)$ are the energy- and voltage-dependent transmission coefficients of the junction, defined in Eq. (A14) in Appendix A, and $n_{L,R}$ are the distribution functions of the left (L) and right (R) electrodes, also defined in Appendix A. $G(V)$ can be approximated at low enough voltages by the linear-response formula

$$G(V) \simeq G_0 T(E = eV, 0) = G_0 \mathcal{T}(E = eV). \tag{2}$$

We show in Figs. 1 and 2 the transmission coefficients $\mathcal{T}(E)$ for all the gold and platinum junctions simulated. Notice that we have taken the Fermi energy of the semi-infinite electrodes at equilibrium as the reference energy. Overall, we find that the zero-voltage conductance $G(0)$ is of order G_0,

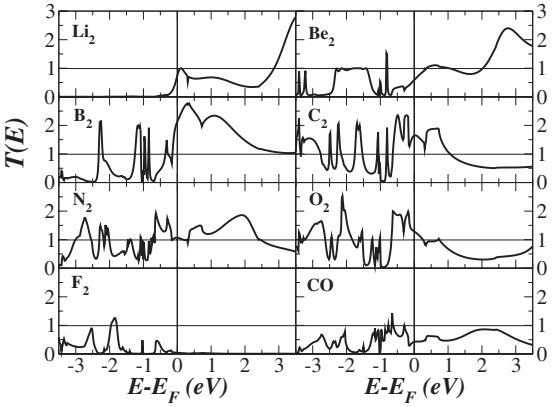

FIG. 2. Transmission coefficients at zero voltage as a function of energy for a number of first-row diatomic molecules and CO attached to (001) platinum electrodes. The geometry of the junctions has been relaxed in this case.

with the only exception of the platinum-F_2 junction. Further, all the transmission coefficients are rather smooth at positive energies while they show peaks in a range of energies below E_F. These peaks do not correspond to molecular states but rather to the *d*-band conduction channels at the electrodes and are naturally located either a few eV below E_F for gold or extend up to E_F for platinum. In this last case the *d* channels can also affect the zero-bias conductance and increase it if they are also coupled to the molecular states (in the same way platinum chains can give a conductance greater than $1G_0$).

A closer look at Fig. 1 shows that $\mathcal{T}$ for gold junctions is either a plateau (as in Li_2, Be_2, and F_2) or the sum of a plateau and a broad resonance (in B_2, C_2, N_2, O_2, and C). The broad resonances are due to the coupling between the two *p* orbitals perpendicular to the transport direction and the *d* states of the gold atom that can couple to them by symmetry, which can be seen by the fact that the transmission on these peaks reaches more than 2. This transmission adds up to the background due to the coupling of the *s* and *pz* states, which around the Fermi-level couple mainly to the *s* state of gold and therefore can have a maximum value of 1. The low-voltage conductances are close to G_0 for Li_2 and F_2 while they are of order $0.3-0.7G_0$ for Be_2, C_2, N_2, and CO, and of order $1.5-2G_0$ for B_2 and O_2.

The transmission coefficients of platinum junctions in Fig. 2 show a slightly more complex structure but are still pretty smooth and show no sign of the narrow resonances that mark the tunneling regime. For platinum, Li_2 and N_2 show conductances of about G_0 while Be_2 and CO have about half a conductance quantum, and B_2, C_2, and O_2 have conductances in the range $1.5-2G_0$. The conductance of F_2 is below $0.1G_0$. Our results for CO agree with a previous simulation preformed by Strange *et al.*[23] but fail to reproduce the peak at $1G_0$ shown in the experimental conductance histograms.[18] As a side remark, we should point out that we have found that the conductance of the diatomic molecule between platinum electrodes may increase or decrease by even a factor of 2 depending on its placement and orientation. The great dependence of the conductance on the structural configuration in the case of platinum is basically due to two reasons. On one hand the presence of the pyramids of four atoms between the molecule and the leads, which we also relax, give additional degrees of freedom and varies to a larger extent the structure of the junction as compared to the gold case where only the surfaces were present and were not relaxed. On the other hand the presence of the *d* states at the Fermi level makes the junction very sensitive to structural changes since they can couple or decouple to molecular states depending on the distance and orientation of the molecule.

III. ANALYTICAL MODELS

Caroli's model in its simplest form is depicted schematically in Fig. 3. It consists of two identical semi-infinite chains, called L and R electrodes, which sandwich a free-standing atom (M) so that three of them are initially unconnected. The chains have a single orbital per atom of energy ε; electrons can hop between atoms via the Hamiltonian matrix element t. The three pieces are initially held at the same bias voltage and the common Fermi energy E_F of the unbiased chains is taken as the reference energy. Since the chains are semi-infinite, they can be regarded as reservoirs of electrons, subjected to a given equilibrium chemical potential $\mu_{L,R}$, whose energy-level population is described by the Fermi distribution functions $n_{L,R}$. The central atom is held initially in thermodynamic equilibrium by its contact to a third reservoir at the arbitrary chemical potential $\mu_T = eV_T$. This determines the equilibrium distribution of the atom n_M and therefore its population. The whole system is subsequently biased by a voltage V so that the chemical potentials of the chains is shifted to $\mu_{L,R} = \pm eV/2$ while the chemical potential at the atom can still be left equal to the initial value, although it is physically more reasonable to reset it to the average between μ_L and μ_R. Notice that the three pieces stay initially in equilibrium since they are unconnected. Later on, the central atom is connected to the electrodes by adiabatically switching on the hopping integrals between them until they reach their final value t_M. We assume that the system is able to reach an stationary nonequilibrium state long time afterward,[24] where there is a total bias voltage between the electrodes equal to V that induces a finite electron current. It is important to stress that the charge population at the atom is determined by its contact to three reservoirs, each at a different chemical potential. Notice furthermore that while the coupling to the chains is controlled by t_M, the coupling to the third reservoir cannot be modulated so that the flow of electrons between it and the atom is completely transparent.

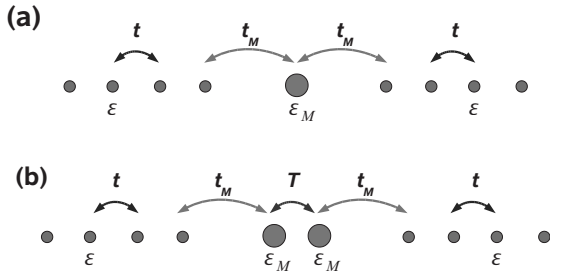

FIG. 3. (a) Two chains made up of P atoms ($P \to \infty$), connected to a central atom by a hopping matrix element t_M. Each of the atoms in the chains has a single orbital with atomic energy ε; electrons in the chains hop from one atom to the next via the hopping integrals t. The central atom has a single orbital of energy ε_M. (b) Two atomic chains connected to a diatomic molecule. Each atom in the molecule has a single orbital of energy ε_M; electrons hop between the two orbitals via the intramolecular hopping integral T.

This model can easily be solved analytically using the machinery of the nonequilibrium Green's functions formalism[25,26] (see Appendix A for a thorough algebraic derivation). Figure 4 shows the results for the density of states at the atom

$$\rho_M(\omega) = -\frac{1}{\pi}\mathrm{Imag}[g^R_{MM}(\omega)], \tag{3}$$

where g^R_{MM} is the retarded Green's function at the central atom, which is defined in Appendix A. The figure also shows the conductance $G(V)$, which has been computed in this case

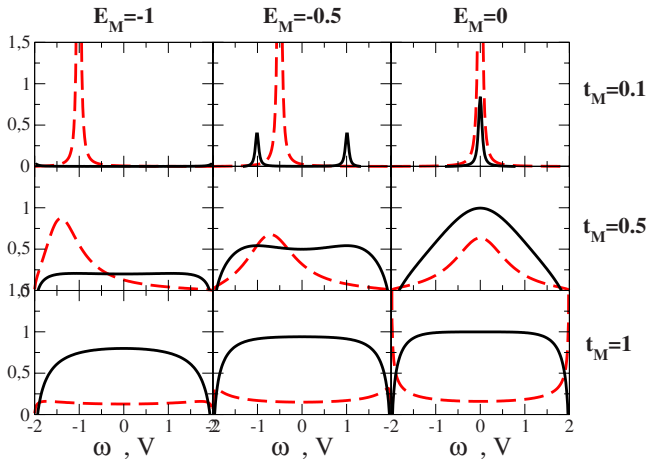

FIG. 4. (Color online) Conductance as a function of voltage (solid black curves) and density of states at the atom at zero voltage as a function of energy (dashed red curves), for Caroli's model. The nine panels displayed correspond to different choices of the parameters t_M and ε_M.

performing the numerical derivative of the current through the junction, to access the high-voltage behavior.

Notice that in this model the position of the HOMO/LUMO levels with respect to the Fermi energy of the electrodes (taken as 0) is given by the atomic energy ε_M while the hopping integral t_M denotes the strength of the HOMO/LUMO hybridization with the electrodes. The hybridization causes two important and well-known effects on the bare atomic level ε_M. First, it renormalizes it, e.g., the level changes its energy. Second, it broadens it since now an electron initially placed at the atomic level can hop back and forth to the electrodes, and hence the atomic state acquires a finite lifetime. These two effects are readily seen in ρ_M, whereby the initial deltalike peak corresponding to the atomic states moves and broadens to a resonance. The resonance is sharp if t_M is much smaller than t, or broad if t_M and t are of the same order of magnitude. What we wish to stress here is that the extent of this broadening also determines the behavior of the conductance of the junction.

Figure 4 illustrates how the different regimes of a junction manifest in the DOS and the conductance and how these regimes are controlled by the basic parameters of the model. In all these cases we chose $\varepsilon=0$ and $t=1$. The top three panels correspond to the resonant tunneling regime. Notice that this regime is seen even for values of the hybridization t_M as large as 0.2. This regime is characterized by a sharp resonance in the DOS, located at the energy position of the molecular orbital ε_M. Additionally, sharp resonances appear in the conductance at different voltages, whose maximum height cannot exceed G_0. The low-voltage conductance is very small except if the molecular orbital is pinned to the Fermi energy in which case $G \simeq G_0$. We stress that the molecular level must be fine tuned to the Fermi energy to achieve sizable values of the conductance. It is important to stress again that the resonant tunneling regime is achieved by values of t_M which are smaller, *but not much smaller*, than t. Just a factor of 5 is enough to place a junction within it.

The bottom panels in Fig. 4 correspond to highly transparent junctions, which corresponds to values of $t_M \simeq 1$. The molecular orbital is in this case fully hybridized with the conduction channels at the electrodes. The DOS is very broad and has a width of the order of the bandwidth of the conduction channels at the electrodes. More importantly, the conductance is very flat and its height is very close to G_0. Notice that this happens for a wide range of positions of the molecular orbital ε_M. Therefore, if the hybridization between the molecular orbital and the conduction channels is large, then there is no need whatsoever to fine tune the position of the molecular orbital. In other words: when $t_M \simeq 1$, the molecular orbital is always tuned, provided it is initially located within the band of the conduction channels at the electrodes. This is one of the central results in this paper.

The middle panels in Fig. 4 show the situation for junctions of intermediate transparency, The DOS reflects this crossover behavior, where a resonance has already been developed but still has a large width. The conductance is very flat but we point that its height has a stronger dependence on the position of the molecular level than was the case of the highly transparent junction.

It is fortunate that some *ab initio* simulation codes[22] allow to make approximate estimates of the physical parameters that appear in Caroli's model. We have indeed recently performed such estimates for a constriction consisting of platinum electrodes bridged by H_2 molecules. We found that in this case $t \sim t_M \sim 5$ eV (e.g., $t_M/t \sim 1$) and that the antibonding state of the molecule was located within the *s-d*-band complex of platinum.[15] We hence ascribed that junction to the highly transparent regime, driven by the large value of t_M. Most of the junctions that we have simulated in this paper, on the other hand, correspond to the crossover regime, where the conductance is of order G_0 but where its exact value has a significant dependence on the exact position of the molecular orbital. This is also the case of the benzene junctions discussed by Kiguchi *et al.*[17]

To make a closer contact with experiments on diatomic molecules, we have performed a slight modification of Caroli's model that we call the diatomic model. In it, the central atom is replaced by a diatomic molecule as depicted in Fig. 1(b). The nice feature of this model is that on the one hand, it accounts for both HOMO and LUMO levels and on the other, it is also easily solved analytically (the algebra is relegated to Appendix B). This model can be applied directly to the case of the platinum-H_2 constriction, where we showed that the electronic conduction is carried by the antibonding state of the molecule, which is strongly hybridized to the platinum conduction bands while the bonding state lies slightly below the edge of the platinum conduction band and hence does not participate in the chemical bond, showing up as a sharp resonance in the DOS.[15] As stated above, we estimated that for this case $t_M \sim t \sim 5$ eV ($t_M/t \sim 1$) while T was slightly larger, about 6 eV ($T/t \sim 1-1.5$).

We display in Fig. 5 the results of the diatomic model for the DOS at the left atom in the molecule and for $G(V)$ for the case where $T=1.5$, and where the bonding state lies below the conduction-band edge and hence shows up as a sharp resonance in the DOS. We again find that when t_M is much smaller than t, both the DOS and G display resonant behavior, whereby the conductance is always very small, except for specific (usually too large) voltages, or when the anti-

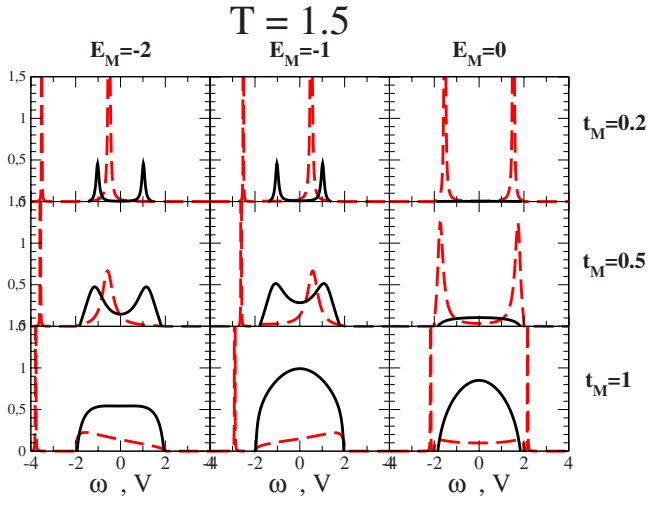

FIG. 5. (Color online) Conductance as a function of voltage (solid black curves) and density of states at the atom as a function of energy (dashed red curves) for the diatomic molecule model. The nine panels displayed correspond to different choices of the parameters t_M and ε_M. The parameter T is set to 1.5 in all cases.

bonding state is finely positioned at the Fermi energy. On the contrary, when $t_M \sim t$, the resonance broadens and the conductance has long plateaus with values close to G_0. The results that compare best to our simulation data for the DOS at the molecule in the platinum-H_2 constriction (see Fig. 3 in Ref. 15) correspond to the middle panel in the bottom row. Hence we expect that this model can describe correctly the platinum-H_2 constriction if we use the parameters $T \sim 1.5$, $t_M \sim 1$, and $\varepsilon_M \sim -1$. Notice that the conductance indeed displays a value close to G_0.

A final note in this section relates to the large variability in the conductance obtained experimentally in BDT/gold junctions. We remind that the voltage at which the conductance resonances depends strongly on the energy position of the molecular orbital for junctions belonging to the resonant tunneling regime. In other words, the value of the measured conductance depends strongly on the details of the orbital and its bonding for this type of junctions. On the contrary, since the conductance has a weak dependence on the details of the molecular orbital for highly transparent junctions, we expect that the experimental variability must be suppressed for them.

IV. ANALYSIS OF BENZENE AND BENZENE-DITHIOLATE JUNCTIONS

Benzene and benzene-dithiol are conjugated molecules whose HOMO and LUMO states correspond to π-bonded p orbitals, which are delocalized throughout the whole molecule. BDT/gold structures are archetypical molecular junctions, which are used as templates against which both theory and experiments are benchmarked. Experimental data show always small conductance values, which range from one to three orders of magnitude smaller than G_0, depending on the experiment. Theoretical results tend to shed larger values for G, typically on the order of 0.05 to 0.1 G_0. This discrepancy

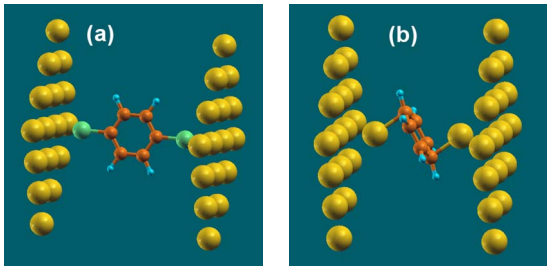

FIG. 6. (Color online) Geometry of (a) benzene-dithiolate/gold and (b) benzene/gold junctions. The drawings show the last layer of gold atoms at each electrode and the carbon, hydrogen, and sulfur atoms of the molecules. (b) also shows the gold apex atoms attached to the gold flat surfaces.

is usually attributed to a poor description of electronic correlations by the theoretical models.[27] BDT/gold junctions therefore seem to belong to the resonant tunneling regime described in the previous section. Interestingly, benzene/platinum junctions are highly conductive,[17] showing values of G on the order of G_0, which indicates that these junctions belong to the intermediate to high transparency regime of Caroli's model. It is therefore important to understand better the contrasting behavior of these seemingly similar junctions.

In order to do so, we have simulated BDT molecules attached to (001) flat gold surfaces. BDT molecules attach via the thiolate groups, such that the sulfur atoms are placed in hollow sites at each side, as shown in Fig. 6(a). We have set a sulfur/gold distance of 2 Å, such that the junction is slightly stretched. We have also simulated benzene molecules attached to (001) gold surfaces. The surfaces are initially flat but we have placed an additional gold atom on top of each of them to provide for a preferred anchoring site. Benzene molecules bind to these electrodes via the π-conjugated molecular orbitals, yielding a geometry for the junction such as that shown in Fig. 6(b). We have set a distance of 5.0 Å between the two apex gold atoms, which is again slightly longer than the equilibrium distance of the junction. We note that there is no direct hybridization between gold orbitals at each side of the junction for such a distance, which is confirmed by negligible transmission coefficients $\mathcal{T}(E)$. Upon relaxation of forces, we have found that the center of the benzene plane is tilted in such a way to maximize the bonding between the π orbitals and the apex gold atoms.

The transmission coefficients of both junctions are plotted in Figs. 7(a) and 8(a). We find that they both show resonances, whose width allows to classify them in the intermediate transparency regimes at first sight. Consequently, the effective hybridization between the HOMO/LUMO levels and the conduction channels is neither too large nor too small. We therefore expect that the conductance must have a relatively strong dependence on the details of the junctions. By analyzing the projected density of states in Figs. 7(b)–7(d) and 8(b)–8(d) it is also possible to determine which atomic orbitals contribute most to the HOMO and LUMO as well as how localized these are.[28]

Our simulations of the benzene-dithiolate/gold junctions yield a zero-voltage conductance of about $0.1G_0$. These junc-

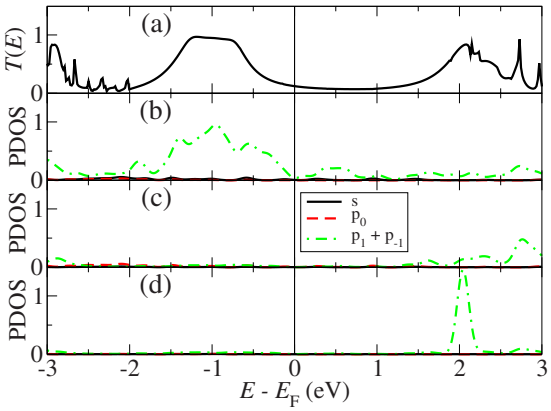

FIG. 7. (Color online) (a) Transmission coefficients $\mathcal{T}(E)$, (b) densities of states projected on the sulfur atoms, (c) the contacting carbon atoms, and (d) the internal carbon atoms for the benzene-dithiolate/gold junction in Fig. 6(a).

tions show two main peaks, placed 1 eV below and 2 eV above the Fermi level, respectively. This means that their zero-voltage conductivity is mostly determined by the HOMO, which is mainly made of the $p_{\pm 1}$ states of sulfur, as can be seen in Fig. 7(b). Such states are perpendicular both to the transport direction and to the BDT molecule. They could only couple to the s or $p_{\pm 1}$ states of carbon in the molecular backbone for symmetry reasons. This is not the case however: Figs. 7(c) and 7(d) show that these carbon states do not hybridize with the sulfur states and are actually located at different energies. As a consequence, those electrons placed at the HOMO state see an effective tunnel barrier to hop from one sulfur atom to the other. This tunnel barrier is not too long however since the distance between the sulfur atoms is not large. The outcome is that the HOMO resonance is not too narrow and reaches a transmission of almost 1. The LUMO is in contrast, localized on the carbon atoms in the molecular backbone, as can be seen in Fig. 7(d). This is in good agreement with previous calculations.[29]

The HOMO and LUMO resonances of the benzene/gold junctions are placed at −2 and +1 eV, respectively, which

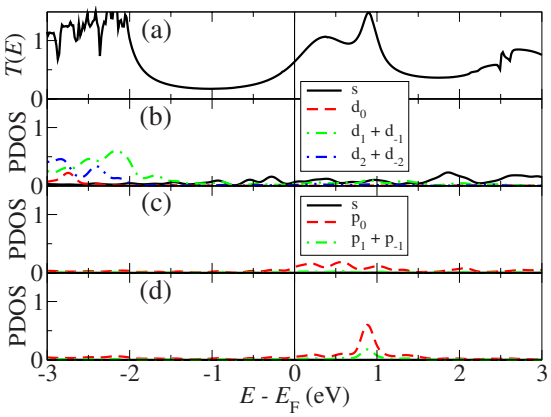

FIG. 8. (Color online) (a) Transmission coefficients $\mathcal{T}(E)$, (b) densities of states projected on the contacting gold atoms, (c) the contacting carbon atoms, and (d) the internal carbon atoms for the benzene/gold junction in Fig. 6(b).

means that the zero-voltage conductivity is in this case mainly determined by the LUMO. Notice that the geometry of this junction is such that the π-conjugated orbitals hybridize directly with the conduction channels at the electrodes. Consequently, the LUMO resonance in the density-of-states and transmission coefficients is broader than in the case of benzene-dithiolate junctions, as is shown in Fig. 8. Superimposed to the LUMO resonance, there exists a sharper additional peak, which is produced by other localized states of the molecular backbone. Notice that in this case it is not so easy to separate p orbitals parallel or perpendicular to the molecular backbone because the benzene molecule is tilted. The HOMO resonance in the density-of-states and transmission coefficients is contributed by states at the apex gold atoms, which give rise to molecular states similar to the previous sulfur states of benzene-dithiolate junctions.

By performing a careful analysis of the alignment of molecular levels before and after adsorption to the gold surfaces it is also possible to determine how the molecular levels arrange after coupling to the electrodes. We calculate the energy alignment before coupling by using a unit cell with the isolated molecules or a gold slab and a hydrogen molecule away enough to define a common reference. We take as an approximation to the gold work function the Fermi energy obtained for a slab of five gold layers. In the BDT case we find that both the HOMO and LUMO, which are very close in energy, lie below the gold Fermi energy. This happens because the HOMO of the benzene-dithiol becomes the LUMO of BDT when it looses the hydrogens attached to the sulfur atoms. When the BDT molecule and the gold electrode get together such levels move upward[30] and the highest level below E_F gets pinned at the Fermi energy so that the molecule ends up winning a bit of charge after coupling (30.58e vs 30.00e for the neutral BDT, obtained from the Mulliken populations). Coupling to the gold surfaces resembles attachment to hydrogen atoms and therefore the resonance at the Fermi energy can be considered the HOMO of the extended molecule, which is separated ~3 eV from the LUMO. This gap is similar to the HOMO-LUMO gap of benzene-dithiol, which is 3.32 eV. In the case of the benzene molecule the HOMO-LUMO gap is bigger (4.25 eV) and the LUMO lies above but close to the Fermi energy so that when the molecule and the gold slab couple the LUMO is pinned at E_F and the molecule ends up winning charge (40.63e vs 40.00e for the neutral molecule) as a consequence of the partial filling of this level.

The reactivity of the thiolate groups is therefore detrimental of the conductivity of benzene-dithiolate junctions. In other words, BDT molecules attach to the electrodes via the thiolate groups, yielding a junction geometry where the HOMO and LUMO do not bind to the conduction channels. The transmission coefficient of this molecule near the HOMO resonance can be explained by using the same simple model employed in the case of alkanes[31] by realizing that such state is in reality composed of two almost degenerated states located on the sulfur atoms and weakly coupled through the benzene ring. By using a simple two-level system as the one shown in Fig. 1(b) it is possible to derive the following formula for the transmission:

$$T(E) = \frac{4\Gamma_L\Gamma_R T^2}{[(E-\varepsilon_M)(E-\varepsilon_M) - \Gamma_L\Gamma_R - T^2]^2 + [(E-\varepsilon_M)\Gamma_R + (E-\varepsilon_M)\Gamma_L]^2}, \tag{4}$$

where Γ are the gamma matrices, defined as $\Gamma = t_M * \rho$, where ρ is the density of states in the leads, which in the case of gold can be taken as constant around the Fermi level due to the presence of only a broad *s* band. By using $\varepsilon_M = -1$, $\Gamma_L = \Gamma_R = 0.5$, and $T = 0.53$ (everything in eV) we obtain the curve shown in Fig. 9, which looks very similar to the HOMO obtained in the *ab initio* computations. Notice this is not a Lorentzian curve (it is composed instead of two Lorentzians) and its width can therefore not be univocally assigned to the coupling to the leads.

V. CONCLUSIONS

We have performed simulations of a number of molecular junctions, where (001) gold or platinum electrodes sandwich first-row diatomic molecules. We have found that these junctions are highly conductive, which is manifested both in large values of the conductance and in smooth transmission coefficients $\mathcal{T}(E)$. We have used Caroli's model to argue that this is a generic feature of the transparent regime of a junction, which is driven by a high hybridization between the delocalized molecular orbitals in the molecule and the conduction levels at the electrodes.

ACKNOWLEDGMENTS

J.F. acknowledges conversations with J. van Ruitenbeek and O. Tal, as well as their sharing their results with us prior to submission. This research has been funded by the Spanish Government (Project No. FIS2006-12117).

APPENDIX A: CAROLI'S MODEL

It is convenient from a mathematical point of view to split the total Hamiltonian in two pieces: the unperturbed Hamiltonian of the total system $\mathcal{H}_0$ and the perturbation that drives the system out of equilibrium $\mathcal{H}_1$. We use the basis of atoms in the system, whose $2P+1$ states we denote by $|i\rangle$. Then the Hamiltonians can be written as the following matrices:

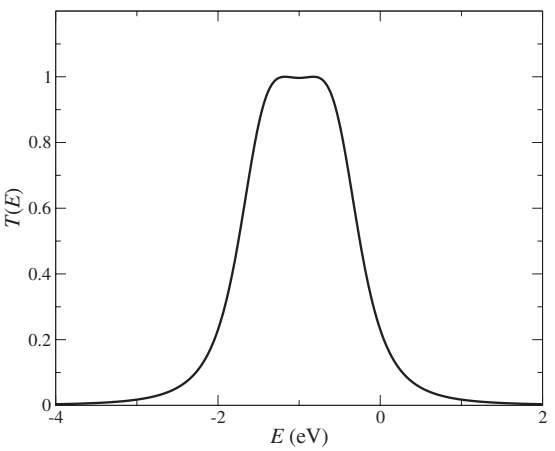

FIG. 9. HOMO resonance calculated with a two-level system, where $\varepsilon_M = -1$ eV, $\Gamma_L = \Gamma_R = 0.5$ eV, and $T = 0.53$ eV.

$$\mathcal{H}_0 = \begin{pmatrix} \hat{H}_L & 0 & 0 \\ 0 & \varepsilon_M & 0 \\ 0 & 0 & \hat{H}_R \end{pmatrix} \quad \mathcal{H}_1 = \begin{pmatrix} 0 & \hat{T}_L & 0 \\ \hat{T}_L^\dagger & 0 & \hat{T}_R^\dagger \\ 0 & \hat{T}_R & 0 \end{pmatrix}, \tag{A1}$$

where $H_{L,R}$ are $P \times P$ tridiagonal matrices of the form

$$\hat{H}_{L,R} = \begin{pmatrix} . & . & . & . & . & . & . & . \\ . & 0 & t & \varepsilon \pm eV/2 & t & 0 & . & . \\ . & . & 0 & t & \varepsilon \pm eV/2 & t & 0 & . \\ . & . & . & . & . & . & . & . \end{pmatrix} \tag{A2}$$

and $\hat{T}_L^\dagger = (\ldots, 0, 0, t_M)$ and $\hat{T}_R^\dagger = (t_M, 0, 0, \ldots)$ are P-dimensional vectors.

The retarded and advanced Green's functions of the unperturbed system can be calculated through the equations

$$[\omega^\pm - \mathcal{H}_0]\mathcal{G}_0^{R,A}(w) = \mathcal{I}, \tag{A3}$$

where $\omega^\pm = \omega \pm i\delta$, δ being an infinitesimal number. Notice that $\mathcal{G}$ are also huge matrices of size $(2P+1) \times (2P+1)$.

This large set of coupled equations can actually be reduced enormously by Gaussian elimination of the atoms in the electrodes until only three states remain, $|L\rangle, |M\rangle, |R\rangle$. The resulting 3×3 matrix Green's functions are called F to avoid confusing them with the conductance, which is denoted by G. Their matrix elements (R/A superindices are henceforth dropped when there is no danger of confusion)

$$F_0 = \begin{pmatrix} g_L & 0 & 0 \\ 0 & g_M & 0 \\ 0 & 0 & g_R \end{pmatrix}. \tag{A4}$$

Here $g_{L,R}$ are the surface Green's function of the electrodes and in our one-dimensional model they are equal to

$$g_{L,R}^{R,A} = \frac{2}{\omega^\pm - \varepsilon + \sqrt{(\omega^\pm - \varepsilon)^2 - 4t^2}}. \tag{A5}$$

To simplify matters, we will take henceforth $\varepsilon = 0$ and t as the energy unit. We also define a *lesser* Green's function that carries information of the electron occupation in each piece,

$$F_0^< = \begin{pmatrix} g_L^< & 0 & 0 \\ 0 & g_M^< & 0 \\ 0 & 0 & g_R^< \end{pmatrix}, \tag{A6}$$

where each $g^<_{L,R,M}(\omega)$ is written in terms of the density of states $\rho_{L,M,R}$ and the Fermi distribution function $n_{L,M,R}$ of each unconnected piece, as $g_i^<(\omega)=2\pi i\rho_i(\omega-eV_i)n(\omega-eV_i)$.

Then the Keldish formalism[21,25] provides a simple recipe to compute the Green's functions of the final system in the steady state,

$$F^R = [(G_0^R)^{-1} - \mathcal{H}_1]^{-1} = \begin{pmatrix} g_{LL}^R & g_{LM}^R & g_{LR}^R \\ g_{ML}^R & g_{MM}^R & g_{MR}^R \\ g_{RL}^R & g_{RM}^R & g_{RR}^R \end{pmatrix},$$

$$F^< = G^R[G_0^R]^{-1}G_0^<[G_0^A]^{-1}G^A = \begin{pmatrix} g_{LL}^< & g_{LM}^< & g_{LR}^< \\ g_{ML}^< & g_{MM}^< & g_{MR}^< \\ g_{RL}^< & g_{RM}^< & g_{RR}^< \end{pmatrix}. \tag{A7}$$

These equations can easily be solved analytically with the following result for the retarded/advanced Green's function:

$$t_M^2 F = \frac{1}{D}\begin{pmatrix} \Sigma_L(\omega-\varepsilon_M-\Sigma_R) & t_M\Sigma_L & \Sigma_L\Sigma_R \\ t_M\Sigma_L & t_M^2 & t_M\Sigma_R \\ \Sigma_L\Sigma_R & t_M\Sigma_R & \Sigma_R(\omega-\varepsilon_M-\Sigma_L) \end{pmatrix}, \tag{A8}$$

where $\Sigma_{L,R}=t_M^2 g_{L,R}$ and $D=\omega-\varepsilon_M-\Sigma_L-\Sigma_R$. Likewise, $F^<$ can be written as the sum of the following three matrices:

$$L = \frac{2\pi i\rho_L n_L}{|D|^2}\begin{pmatrix} |\omega-\varepsilon_M-\Sigma_R|^2 & t_M(\omega-\varepsilon_M-\Sigma_R^R) & \Sigma_R^A(\omega-\varepsilon_M-\Sigma_R^R) \\ t_M(\omega-\varepsilon_M-\Sigma_R^A) & t_M^2 & t_M\Sigma_R^A \\ \Sigma_R^R(\omega-\varepsilon_M-\Sigma_R^A) & t_M\Sigma_R^R & |\Sigma_R|^2 \end{pmatrix},$$

$$R = \frac{2\pi i\rho_R n_R}{|D|^2}\begin{pmatrix} |\Sigma_L|^2 & t_M\Sigma_L^R & \Sigma_L^R(\omega-\varepsilon_M-\Sigma_L^A) \\ t_M\Sigma_L^A & t_M^2 & t_M(\omega-\varepsilon_M-\Sigma_L^A) \\ \Sigma_L^A(\omega-\varepsilon_M-\Sigma_L^R) & t_M(\omega-\varepsilon_M-\Sigma_L^R) & |\omega-\varepsilon_M-\Sigma_L|^2 \end{pmatrix},$$

$$t_M^2 M = \frac{2\pi i\rho_M n_M}{|g_M D|^2}\begin{pmatrix} |\Sigma_L|^2 & t_M\Sigma_L^R & \Sigma_L^R\Sigma_R^A \\ t_M\Sigma_L^A & t_M^2 & t_M\Sigma_R^A \\ \Sigma_R^R\Sigma_L^A & t_M\Sigma_R^A & |\Sigma_R|^2 \end{pmatrix}. \tag{A9}$$

These lesser Green's functions enter the calculation of the electronic charge and current. For instance, the charge at the atom N_M can be written as follows:

$$N_M = \int \frac{d\omega}{2\pi i} g_{MM}^<(\omega) = \int \frac{d\omega}{2\pi}|g_{MM}^R|^2\left(\Gamma_L n_L + \Gamma_R n_R + \frac{\Gamma_M}{|t_M g_M|^2} n_M\right). \tag{A10}$$

This formula for the charge can be rewritten in terms of the conventional expression for the equilibrium state

$$N_{eq} = -\int \frac{d\omega}{\pi}\mathrm{Im}[g_{MM}^R]n_L \tag{A11}$$

plus an explicit nonequilibrium term

$$N_{noneq} = \int \frac{d\omega}{2\pi}|g_{MM}^R|^2\Gamma_R(n_R-n_L) + \int \frac{d\omega}{2\pi}|g_{MM}^R|^2\frac{\Gamma_R}{|t_M g_M|^2}(n_M-n_L), \tag{A12}$$

where

$$\Gamma_{L,R} = i(\Sigma_{L,R}^R - \Sigma_{L,R}^A) = 2\pi t_M^2\rho_{L,R}(\omega-eV_{L,R})$$

and likewise

$$\Gamma_M = 2\pi t_M^2\rho_M(\omega-eV_T).$$

The current traversing the left contact is computed via the formula

$$I_{LM} = -\frac{2et_M}{\hbar}\int \frac{d\omega}{2\pi}(g_{LM}^< - g_{ML}^<), \tag{A13}$$

which can be written as a sum of the following two contributions:

$$I_{leads} = -\frac{G_0}{e}\int d\omega |g^R_{MM}|^2 \Gamma_L \Gamma_R (n_L - n_R)$$
$$= -\frac{G_0}{e}\int d\omega T(E=\hbar\omega, V)(n_L - n_R),$$

$$I_{atom,L} = -\frac{G_0}{e}\int d\omega |g^R_{MM}|^2 \frac{\Gamma_L \Gamma_M}{t_M^2} n_M. \quad \text{(A14)}$$

Notice that the current traversing the right contact can be written as the sum of I_{leads} plus $I_{atom,R}$ where

$$I_{atom,R} = -\frac{G_0}{e}\int d\omega |g^R_{MM}|^2 \frac{\Gamma_R \Gamma_M}{t_M^2} n_M. \quad \text{(A15)}$$

Since these atomic contributions apparently break the conservation of charge, $I_{atom,(L,R)}$ are usually dropped [as is the second term in Eq. (15)]. In other words, the total current I is approximated by I_{leads}.

APPENDIX B: DIATOMIC MOLECULE MODEL

The unperturbed Hamiltonian and the perturbation in the diatomic model take the form

$$\mathcal{H}_0 = \begin{pmatrix} \hat{H}_L & 0 & 0 & \\ 0 & \varepsilon_M & T & 0 \\ 0 & T & \varepsilon_M & 0 \\ 0 & 0 & 0 & \hat{H}_R \end{pmatrix}, \quad \text{(B1)}$$

where $H_{L,R}$ are the $P \times P$ tridiagonal matrices described in Appendix A and

$$\mathcal{H}_1 = \begin{pmatrix} 0 & \hat{T}_L & 0 & 0 \\ \hat{T}_L^\dagger & 0 & 0 & 0 \\ 0 & 0 & \hat{T}_R^\dagger & 0 \\ 0 & 0 & \hat{T}_R & 0 \end{pmatrix}. \quad \text{(B2)}$$

After decimating the unwanted degrees of freedom, the unpertubed Green's functions look like

$$F_0^{R,A,<} = \begin{pmatrix} g_L^{R,A,<} & 0 & 0 \\ 0 & \hat{g}_M^{R,A,<} & 0 \\ 0 & 0 & g_R^{R,A,<} \end{pmatrix}, \quad \text{(B3)}$$

where

$$\hat{g}_M^{R,A} = \begin{pmatrix} \omega - \varepsilon_M & -T \\ -T & \omega - \varepsilon_M \end{pmatrix} \quad \text{(B4)}$$

and $\hat{g}_M^< = -1/\pi(\hat{g}_M^R - \hat{g}_M^A) n_M$. The algebra is more tedious but the final result for the retarded Green's function $t_M^2 F$ is the following:

$$\frac{1}{D}\begin{pmatrix} \Sigma_L[(\omega-\varepsilon_M)(\omega-\varepsilon_M-\Sigma_R)-T^2] & t_M\Sigma_L(\omega-\varepsilon_M-\Sigma_R) & t_M T\Sigma_L & T\Sigma_L\Sigma_R \\ t_M\Sigma_L(\omega-\varepsilon_M-\Sigma_R) & t_M^2(\omega-\varepsilon_M-\Sigma_R) & t_M^2 T & t_M T\Sigma_R \\ t_M T\Sigma_L & t_M^2 T & t_M^2(\omega-\varepsilon_M-\Sigma_L) & t_M\Sigma_R(\omega-\varepsilon_M-\Sigma_L) \\ T\Sigma_L\Sigma_R & t_M T\Sigma_R & t_M\Sigma_R(\omega-\varepsilon_M-\Sigma_L) & \Sigma_R[(\omega-\varepsilon_M)(\omega-\varepsilon_M-\Sigma_L)-T^2] \end{pmatrix}, \quad \text{(B5)}$$

where $D=(\omega-\varepsilon_M)(\omega-\varepsilon_M-\Sigma_R-\Sigma_R)-T^2+\Sigma_L\Sigma_R$ and the equation for the current traversing the left link can be written as

$$I_{LM} = -\frac{2e}{h}\int d\omega \Gamma_L \Gamma_R |G^R_{MM'}|^2 (n_r - n_L), \quad \text{(B6)}$$

where the atomic contribution has been neglected again and $G_{MM'}$ refers to the element (2,3) of the retarded Green's function matrix that connects the two atoms in the molecule.

[1] A. Aviram and M. A. Ratner, Chem. Phys. Lett. **52**, 9071 (1974).
[2] M. A. Reed, C. Zhou, C. J. Muller, T. P. Burgin, and J. M. Tour, Science **278**, 252 (1997).
[3] C. P. Collier, E. W. Wong, M. Belohradský, F. M. Raymo, J. F. Stoddart, P. J. Kuekes, R. S. Williams, and J. R. Heath, Science **285**, 391 (1999).
[4] S. Datta, *Electronic Transport in Mesoscopic Systems* (Cambridge University Press, Cambridge, UK, 1995).
[5] G. Binnig, H. Rohrer, Ch. Gerber, and E. Weibel, Phys. Rev. Lett. **49**, 57 (1982).
[6] J. K. Gimzewski and R. Möller, Phys. Rev. B **36**, 1284 (1987).
[7] N. Agrait, J. G. Rodrigo, and S. Vieira, Phys. Rev. B **47**, 12345 (1993).
[8] J. I. Pascual, J. Mendez, J. Gomez-Herrero, A. M. Baro, N. Garcia, and V. T. Binh, Phys. Rev. Lett. **71**, 1852 (1993).
[9] J. M. Krans, J. M. van Ruitenbeek, V. V. Fisun, I. K. Yanson, and

L. J. de Jongh, Nature (London) **375**, 767 (1995).
[10] N. Agrait, A. Levy Yeyati, and J. M. van Ruitenbeek, Phys. Rep. **377**, 81 (2003).
[11] J. Ferrer, A. Martín-Rodero, and F. Flores, Phys. Rev. B **38**, 10113 (1988).
[12] J. Ferrer, Ph.D. thesis, Universidad Autónoma de Madrid, 1990.
[13] R. H. M. Smit, Y. Noat, C. Untiedt, N. D. Lang, M. C. Van Hemert and J. M. van Ruitenbeek, Nature (London) **419**, 906 (2002).
[14] Sz. Csonka, A. Halbritter, G. Mihaly, O. I. Shklyarevskii, S. Speller, and H. van Kempen, Phys. Rev. Lett. **93**, 016802 (2004).
[15] V. M. García-Suárez, A. R. Rocha, S. W. Bailey, C. J. Lambert, S. Sanvito, and J. Ferrer, Phys. Rev. B **72**, 045437 (2005).
[16] K. S. Thygesen and K. W. Jacobsen, Phys. Rev. Lett. **94**, 036807 (2005).
[17] M. Kiguchi, O. Tal, S. Wohlthat, F. Pauly, M. Krieger, D. Djukic, J. C. Cuevas, and J. M. van Ruitenbeek, Phys. Rev. Lett. **101**, 046801 (2008).
[18] O. Tal, M. Kiguchi, W. H. A. Thijssen, D. Djukic, C. Untiedt, R. H. M. Smit, and J. M. van Ruitenbeek, following paper, Phys. Rev. B **80**, 085427 (2009).
[19] We employed single zeta (SZ) and single zeta polarized (SZP) basis sets for gold and platinum, respectively, defined with an energy shift of 0.02 Ry, a real-space grid defined with a cutoff of 200 Ry and the local-density approximation functional. The SZ basis set in the case of gold was enough to reproduce the qualitative trends we look for in this study and to map the simulations to the simple model. In both cases we used fcc leads grown along the 001 direction with nine atoms per section. The extended molecule included two layers of bulk and two or three additional layers on both sides to ensure a smooth transition between bulk and the surfaces. Each calculation had a number of atoms ranging between 85 and 93 depending on whether additional pyramids were included to contact the molecule.
[20] A. R. Rocha, V. M. García-Suárez, S. Bailey, C. Lambert, J. Ferrer, and S. Sanvito, Phys. Rev. B **73**, 085414 (2006).
[21] C. Caroli, R. Combescot, P. Nozieres, and D. Saint-James, J. Phys. C **5**, 21 (1972).
[22] J. M. Soler, Emilio Artacho, Julian D Gale, Alberto García, Javier Junquera, Pablo Ordejón, and Daniel Sánchez-Portal, J. Phys.: Condens. Matter **14**, 2745 (2002).
[23] M. Strange, K. S. Thygesen, and K. W. Jacobsen, Phys. Rev. B **73**, 125424 (2006).
[24] A. Dhar and D. Sen, Phys. Rev. B **73**, 085119 (2006).
[25] L. V. Keldish, Sov. Phys. JETP **20**, 1018 (1965).
[26] M. Wagner, Phys. Rev. B **44**, 6104 (1991).
[27] C. Toher and S. Sanvito, Phys. Rev. B **77**, 155402 (2008).
[28] V. M. García-Suárez and C. J. Lambert, Phys. Rev. B **78**, 235412 (2008).
[29] Y. Xue and M. A. Ratner, Phys. Rev. B **68**, 115406 (2003).
[30] R. Stadler and K. W. Jacobsen, Phys. Rev. B **74**, 161405(R) (2006).
[31] S. Martín, D. Zsolt Manrique, V. M. García-Suárez, W. Haiss, S. J. Higgins, C. J. Lambert, and R. J. Nichols, Nanotechnology **20**, 125203 (2009).